

Adhesion and Retention of a Bacterial Phytopathogen *Erwinia chrysanthemi* in Biofilm-Coated Porous Media

YANG LIU,[†] CHING-HONG YANG,[‡] AND JIN LI^{*†}

Department of Civil Engineering and Mechanics, and Department of Biological Sciences, University of Wisconsin-Milwaukee, Milwaukee, Wisconsin 53201

Received July 10, 2007. Revised manuscript received October 2, 2007. Accepted October 10, 2007.

The goal of this study is to investigate the impact of biofilm physical and biological properties on bacterial transport and deposition in porous media. Experiments were performed in packed columns to examine the removal of *Erwinia chrysanthemi* (Ech3937), a phytopathogen, from the bulk fluid due to its attachment to glass beads coated with *Pseudomonas aeruginosa* biofilms. Two isogenic *P. aeruginosa* strains, PAO1 and PDO300, with different EPS secretion capabilities and EPS compositions, were used to culture biofilms. The Ech3937 transport and distribution in packed columns were studied in both upflow and downflow cell injection modes over a range of solution ionic strengths. The results show that the presence of biofilm strongly interferes with the deposition behavior of Ech3937 in porous media. The spatial variation of deposited Ech3937 cells contradicts the log-linear pattern predicted by the classic filtration theory, indicating that the biofilm physical structure and polymeric interactions between the biofilm EPS and Ech3937 cell surface are the main mechanisms that control bacterial deposition. When the biofilm accumulation is relatively small, bacterial adhesion onto biofilm-coated porous media is mainly inhibited by steric forces. By contrast, cell deposition is enhanced by the reduced porous media porosity when biofilm is more abundant.

Introduction

Bacterial deposition onto biofilm-coated porous media is a crucial phenomenon in various environmental processes, including bioremediation, biofiltration, and pathogen transport in soil and groundwater. Biofilm is an assemblage of microbial cells enclosed in a matrix of extracellular polymeric substances (EPS), which form on surfaces in virtually all aquatic ecosystems that can support microbial growth, e.g., soil, rock, plants, sediments, and filter media (1–3). EPS, a complex mixture of biomacromolecules consisting primarily of polysaccharides and proteins with small but variable amounts of lipids and nucleic acids, can make up to 90% of the organic carbon in a typical biofilm. The EPS constituents contain active sites such as neutral moieties, e.g., saccharide, and ionized moieties, e.g., carboxyl, phosphate, and amino

groups, whose interaction with bacteria changes as a function of solution pH.

The impact of biofilm EPS on bacterial adhesion is determined by a number of factors, including DLVO (Derjaguin Landau Verwey Overbeek) forces, i.e., van der Waals and electrostatic forces (4, 5), hydrophobicity and hydration effects as described by the DLVO-AB model (6, 7), and non DLVO interactions, e.g., polymeric interactions (8–13). Depending on its shape, compressibility, and chemical composition, bacterial surface EPS may encourage adhesion in porous media by polymer bridging between cells and the solid surface (12, 14, 15) or hinder cells to reach the energy minimum by steric interactions (9, 11). Recent atomic force microscopy (AFM) studies also have shown that interaction between biopolymer coated surfaces and bacteria are complex (16, 17).

Biofilms are known to affect the physical and hydrodynamic properties of porous media. Different from the ion-impermeable inorganic porous media surfaces, biofilm formation provides small water channels that can help convey water and chemical solutes while preventing bacteria and colloids that are too large to pass through (18, 19). Biofilms may promote bacterial deposition by physical straining or discourage bacterial adhesion through changes in hydrodynamic conditions caused by extensive biofilm growth (20–22). As biomass accumulates, the reduced bed porosity provides an additional surface area for deposition, which can enhance particle removal (23). Conversely, reduced porosity leads to an increased local flow velocity and shear stress, which can impair the deposition (18, 19).

This study evaluates the transport and deposition of an opportunistic plant pathogen, *Erwinia chrysanthemi*, in porous media under the influence of *Pseudomonas aeruginosa* biofilms with different EPS compositions. *E. chrysanthemi* (*Dickeya dadantii*) causes soft-rot, wilt, and blight diseases on a wide range of plant species (24). *E. chrysanthemi* is a gram negative, facultatively anaerobic, and peritrichously flagellated bacterium isolated from plants; approximately 70% nucleotide identity homologous to *E. coli* K-12 genes (24). *P. aeruginosa* is a gram negative bacterial pathogen that not only causes opportunistic human infection but also infects plants, insects, and nematode (25, 26). *P. aeruginosa* is the dominant pathogen that infects the lungs of cystic fibrosis patients (26). Some clinical isolates of *P. aeruginosa* were reported to cause soft-rot symptoms when inoculated into lettuce, onions, tobacco, and tomatoes. In addition, *P. aeruginosa* is found as a common colonizer of many plants without showing disease symptoms (27). Although no study on mixed biofilm communities of these two organisms has been reported in natural environment so far, the multiple host property of *P. aeruginosa* and the close phylogenetic relationship of the plant pathogen *E. chrysanthemi* to the animal-associated pathogens such as *Escherichia*, *Salmonella*, and *Yersinia*, make it interesting to investigate the biofilm formation and bacterial deposition between these two organisms.

Materials and Methods

Packed-Bed Column Setup. Glass beads with an average diameter of 550 μm (MO-SCI Specialty Products, MO) were used as the porous media for bacterial transport experiments. Cylindrical polycarbonate plastic columns (26 cm long and 2.54 cm internal diameter) were wet-packed with glass beads thoroughly cleaned following the procedure described previously (28). The porosity of the packed glass beads was determined gravimetrically to be 0.4.

* Corresponding author phone: (414) 229-6891; fax: (414) 229-6958; e-mail: li@uwm.edu.

[†] Department of Civil Engineering and Mechanics.

[‡] Department of Biological Sciences.

Biofilm Development. Biofilms were grown in the packed bed using a *P. aeruginosa* wild type strain PAO1 and its isogenic mucoid alginate-overproducing strain with a *mucaA22* mutation, PDO300. The stored bacteria were streaked onto Luria–Bertani (LB) agar plates and incubated at 37 °C overnight. A single colony was then transferred into a LB broth and grown in a shaker incubator at 200 rpm at 37 °C for 20 h. To seed the columns, 150 mL of bacterial suspension with approximately 10⁸ CFU/mL PAO1 or PDO300 cells was fed to the columns at a flow rate of 3.0 mL/min in an upflow mode. After seeding, the system was operated with a 100% recycle for 12 h to facilitate sufficient cell attachment. The bacterial suspension was then replaced with a nutrient solution whose composition was described in a previous paper (29), to support biofilm growth. The system was operated continuously for five days under constant flow rate and flow direction.

Bacterial Strains and Cell Preparation. The column study used the wild type *E. chrysanthemi* 3937 strain (Ech3937) carrying a plasmid nptBROBE-AT that constitutively expresses green fluorescent protein (GFP). Plasmid nptBROBE-AT was constructed by inserting a kanamycin cassette DNA fragment in front of the *gfp* gene of vector pBROBE-AT (30). From our previous study, 95.5% of the Ech3937 cells retained pBROBE-AT derivatives during 12 h of growth in media (31). Ech3937 cells were grown at 28 °C in 30 mL of LB broth supplemented with 50 µg/mL kanamycin while shaking at 200 rpm in a shaker incubator until they reached the stationary phase. Cells were harvested by centrifugation at 3000g and 4 °C for 10 min. The growth medium was decanted and the pellets were resuspended in phosphate buffered saline (PBS) with ionic strengths 165, 16.5, and 1.65 mM, respectively. The centrifugation-resuspension process was repeated three times to remove traces of growth media. A final cell density of approximately 10⁷ cells/mL was obtained by measuring the optical density (OD) of the cell suspension at 600 nm wavelength.

Column Experiments. Three sets of experiments were carried out in the packed bed columns using (i) glass beads without biofilm; (ii) glass beads coated with PAO1 biofilm; and (iii) glass beads coated with PDO300 biofilm. The transport and deposition of Ech3937 cells were compared in 165, 16.5, and 1.65 mM PBS, with upflow and downflow cell injection.

Injection of Ech3937 suspensions began after equilibrating the columns for at least 20 pore volumes (PVs) of bacteria-free background electrolytes at a constant approach velocity of 0.011 cm/s. Approximately 8 PVs of Ech3937 suspension were injected, followed by eluting the columns with another 8 PVs of background solutions. Each PV of the column effluent was collected in 50 mL polystyrene tubes and immediately placed on ice prior to microbiological analysis.

After completing each transport experiment, the column media were dissected into 5 cm long segments to obtain the spatial distribution of retained Ech3937 cells, the biofilm biomass, and their associated EPS. Each 5 cm section of the porous media was placed into a beaker containing 50 mL of PBS. The glass beads bound biofilm and Ech3937 cells were dissociated by ultrasonication (8). All experiments were performed in triplicates at room temperature (20–25 °C). The overall recovery (mass balance) of Ech3937 bacteria was determined by summing the Ech3937 bacteria collected in the effluent and those recovered from the column media.

Bacterial Count and EPS Analysis. Ech3937 recovered from the effluent and column media were counted by fluorescent-activated cell sorting (FACS) analysis with a FACSCalibur flow cytometer (BD Biosciences, CA) equipped with an air-cooled argon-ion laser (15 mW at 488 nm) and a standard filter setup. Ech3937 bacteria were distinguished from *P. aeruginosa* biofilm bacteria by their strong green

fluorescence signal, which was collected in the FL1 channel (530 ± 15 nm). Signals were amplified with the logarithmic mode for forward scattering, side scattering, and fluorescence. The positive control (freshly prepared Ech3937 bacteria in PBS) and the negative control (bacteria-free PBS) were run first, followed by injecting samples through the flow cytometer at a flow rate of 12 µL/s for 1 min. All injections were performed in triplicates and the average was reported.

The biofilm EPS was extracted using the high-speed centrifugation method (32). Carbohydrates were quantified using the phenol–sulfuric acid method described by Dubois (33), with glucose as the standard. Proteins were assayed colorimetrically by a bicinchoninic acid (BCA) protein assay kit (Bio-Rad Laboratories, CA). Uronic acids were measured using the *m*-hydroxydiphenyl sulfuric acid method, with *D*-glucuronic acid as the standard (34).

Electrokinetic Characterization of Bacterial Cells and Glass Beads Surfaces. A ZetaPALS Analyzer (Brookhaven Instruments Corp., NY) was used to measure the cell and smashed glass beads electrophoretic mobility and zeta potential in PBS. The measurements were performed 10 times for each assay.

Determination of Deposition Rate Coefficient. The Ech3937 deposition pattern was analyzed in terms of the deposition rate coefficient, k_d . Assuming uniform biofilm distribution inside each 5 cm segment, k_d can be obtained by using the steady state breakthrough concentration of the cell according to the following equation (35, 36):

$$\ln \frac{C}{C_0} = - \int_0^x k_d(x') \cdot \frac{\epsilon(x')}{U} dx' \quad (1)$$

where C/C_0 is the normalized breakthrough concentration, ϵ is the bed porosity, U is the approach velocity, x is the column depth, and x' is the first derivative of x .

By applying the measured retained Ech3937 bacterial number in each segment, the suspended bacterial concentration inside the column could be obtained, which can be used to evaluate the k_d distribution using the following equation:

$$k_{d_i} = - \frac{U}{\epsilon_i \cdot \Delta x} (\ln \frac{C_i}{C_0} - \ln \frac{C_{i-1}}{C_0}) \quad (2)$$

where i is the number of the segment, $i = 1, \dots, 5$ in this study. C_i is the suspended bacterial concentration at the end of each segment; C_0 is the influent cell concentration; and Δx is the length of each segment (5 cm).

Results

Electrokinetic Potential of Bacterial Cells. Figure S1 (in the Supporting Information) presents the influence of solution ionic strength on the zeta potentials of Ech3937, PAO1, and PDO300 bacterial cells, and bare glass beads. Under the conditions investigated, all three bacterial strains and glass beads exhibited negative zeta potentials and their surface charges became less negative with increasing ionic strength. Under low and medium ionic strengths (1.65 and 16.5 mM), Ech3937 had less negative surface charge than the glass beads, while the surfaces of PAO1 and PDO300 were more negative than the glass beads. The difference of zeta potentials among the bacteria and glass beads became less pronounced under high ionic strength (165 mM).

Biofilm Characterization. The spatial distribution of PAO1 and PDO300 biofilms in the packed columns was investigated by quantifying the biofilm bacteria and major EPS components, i.e., protein and carbohydrate for PAO1 biofilm and protein, carbohydrate, and uronic acid for PDO300 biofilm. As shown in Figure 1, *P. aeruginosa* bacterial cells and their associated EPS were unevenly distributed in the columns and the majority of biofilm bacteria colonized near the

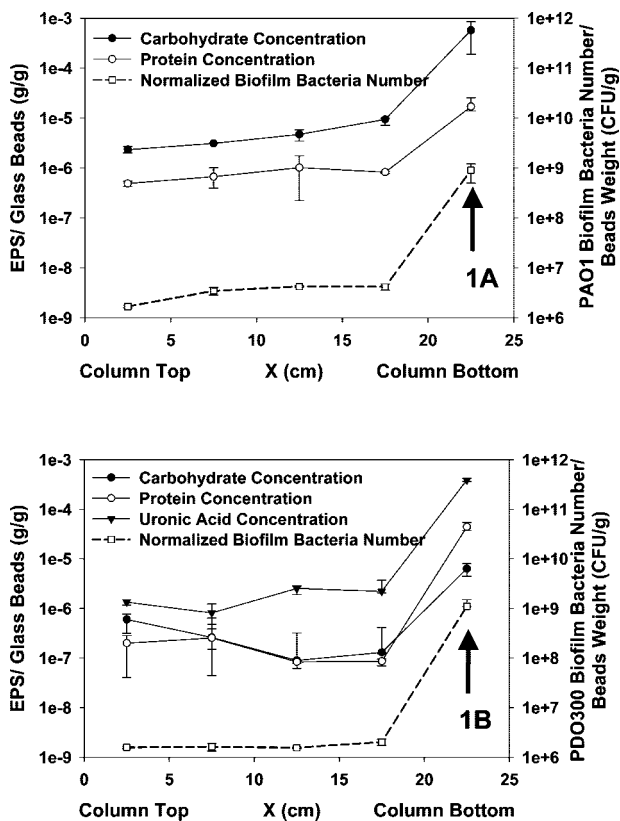


FIGURE 1. Measured biofilm bacterial density, carbohydrate, uronic acid, and protein profiles for PAO1 biofilm (nonmucoid wild-type strain) (1A), and PDO300 biofilm (mucoid alginate-overproducing strain) (1B) along the column length. Error bars represent standard deviations of three replicate experiments; arrows indicate the column section close to nutrient solution injection inlet.

column bottom where the nutrient solution was injected. This type of uneven distribution of biofilm is commonly observed in biofilters and slow sand filters, in which a hypogeal layer or *Schmutzdecke* forms in the top few millimeters of the fine sand layer. The normalized cell density of PAO1 biofilm bacteria was approximately 8.6×10^8 CFU/g beads in the bottom 5 cm segment, and decreased to $1.7\text{--}4.2 \times 10^6$ CFU/g beads for the rest of the column (Figure 1A). Slightly more PDO300 biofilm formed on the column media compared with PAO1 biofilm under the same condition. Colonized PDO300 cell concentration reached 1.1×10^9 CFU/g beads within the bottom 5 cm of the column, and was distributed more uniformly for the rest of the column, with bacterial concentrations ranging from 1.5×10^6 to 2.0×10^6 CFU/g beads (Figure 1B). The EPS concentration profiles along the columns followed trends similar to those of the corresponding PDO300 and PAO1 cells, although slight fluctuations were observed toward the top of the columns.

Ech3937 Breakthrough Curves. The breakthrough curves shown in Figure 2 illustrate the influence of ionic strength, solution injection direction, and biofilm coating on Ech3937 transport. The relative cell densities (C/C_0) in the column outflow are plotted against the number of PVs injected. As shown in Figure 2A and B, similar breakthrough patterns were observed for both upflow and downflow cell injections in clean columns, indicating that the pore fluid injection direction had a negligible impact on cell retention under clean bed condition. In clean columns, the normalized effluent Ech3937 concentration C/C_0 was nearly constant during the course of bacterial injection under low and medium ionic strengths (1.65 and 16.5 mM) with steady breakthrough plateaus. Under high ionic strength (165 mM),

the magnitude of the steady state breakthrough concentration C/C_0 declined, implying the occurrence of a phenomenon known as ripening, caused by deposited bacterial cells serving as favorable sites for subsequent cell attachment.

Figure 2C and D show the Ech3937 breakthrough curves in PAO1 biofilm-coated columns, and Figure 2E and F show the Ech3937 breakthrough curves in PDO300 biofilm-coated columns. The presence of both PAO1 and PDO300 biofilms significantly increased Ech3937 deposition compared with the clean columns. Under identical flow direction and solution ionic strength, higher numbers of Ech3937 bacteria were trapped inside the PAO1 biofilm-coated system than in the PDO300 biofilm-coated system. When the column media was coated with the PAO1 biofilm, ripening was observed under all ionic strengths when the transport experiments were run in the downflow mode; however, the ripening phenomenon was not observed when the flow direction was changed to upflow. With the PDO300 biofilm, ripening occurred under both downflow and upflow.

Changing the pore fluid ionic strength from 1.65 to 165 mM increased the retention of Ech3937 in clean columns and PAO1 biofilm-coated columns; however, increasing the ionic strength did not have a significant impact on the magnitude of the steady state breakthrough plateau in the PDO300 biofilm-coated columns.

Distribution of Ech3937 in the columns. Tables S1–S4 (Supporting Information) and Figure 3 show the calculated Ech3937 deposition rate coefficients k_d as a function of cell travel distance in columns. k_d decreased slightly from the column inlet to the outlet under high ionic strength (165 mM) in clean columns under both flow directions (Figure 3A and B). The slope of the k_d profile increased with decreasing ionic strength, which is a common type of deviation from the spatially constant k_d predicted from the filtration theory under unfavorable conditions (37–39). In this study, the spatial variation of k_d appears to be caused by the heterogeneity in the surface characteristics among the bacterial population (38–42); individual microbes that are more prone to retention were deposited near the column inlet, and those less prone to retention were deposited farther away from the column inlet.

The retention patterns of Ech3937 in biofilm-coated columns differ significantly from those observed in clean columns. As shown in Figure 3C–F, k_d distributions correlate well with the biofilm biomass profiles in the columns, with the highest k_d located within the bottom segment (20–25 cm) of the columns regardless of the flow direction, suggesting that the presence of biofilm strongly interferes with bacterial deposition behavior in porous media. Overall, the cell deposition rate coefficients were higher in PAO1 biofilm-coated columns than those in PDO300 biofilm-coated columns under the same experimental conditions. This observation is consistent with our column effluent breakthrough curves. It is also noted that, except for the column bottom segments where the majority of the biofilms resided, lower k_d was found in both biofilm-coated columns compared with the k_d obtained in clean columns under identical experimental conditions. For instance, under the highest ionic strength (165 mM) and upflow condition, k_d in the top 20 cm of the column was $3 \times 10^{-5}/s$ to $6 \times 10^{-5}/s$ in the PDO300 biofilm-coated column, and $4 \times 10^{-5}/s$ to $1.3 \times 10^{-4}/s$ in the PAO1 biofilm-coated column while k_d equaled $8.3 \times 10^{-5}/s$ to $2 \times 10^{-4}/s$ in the clean column.

Mass Balances. Table S5 (Supporting Information) shows the total mass recovery of the Ech3937 bacteria in the clean column and columns coated with PAO1 and PDO300 biofilm. Mass recovery rates in all experiments were between 86% and 118%. The excellent mass balance indicates that ultrasonication was sufficient to remove Ech3937 from glass beads and biofilm surfaces.

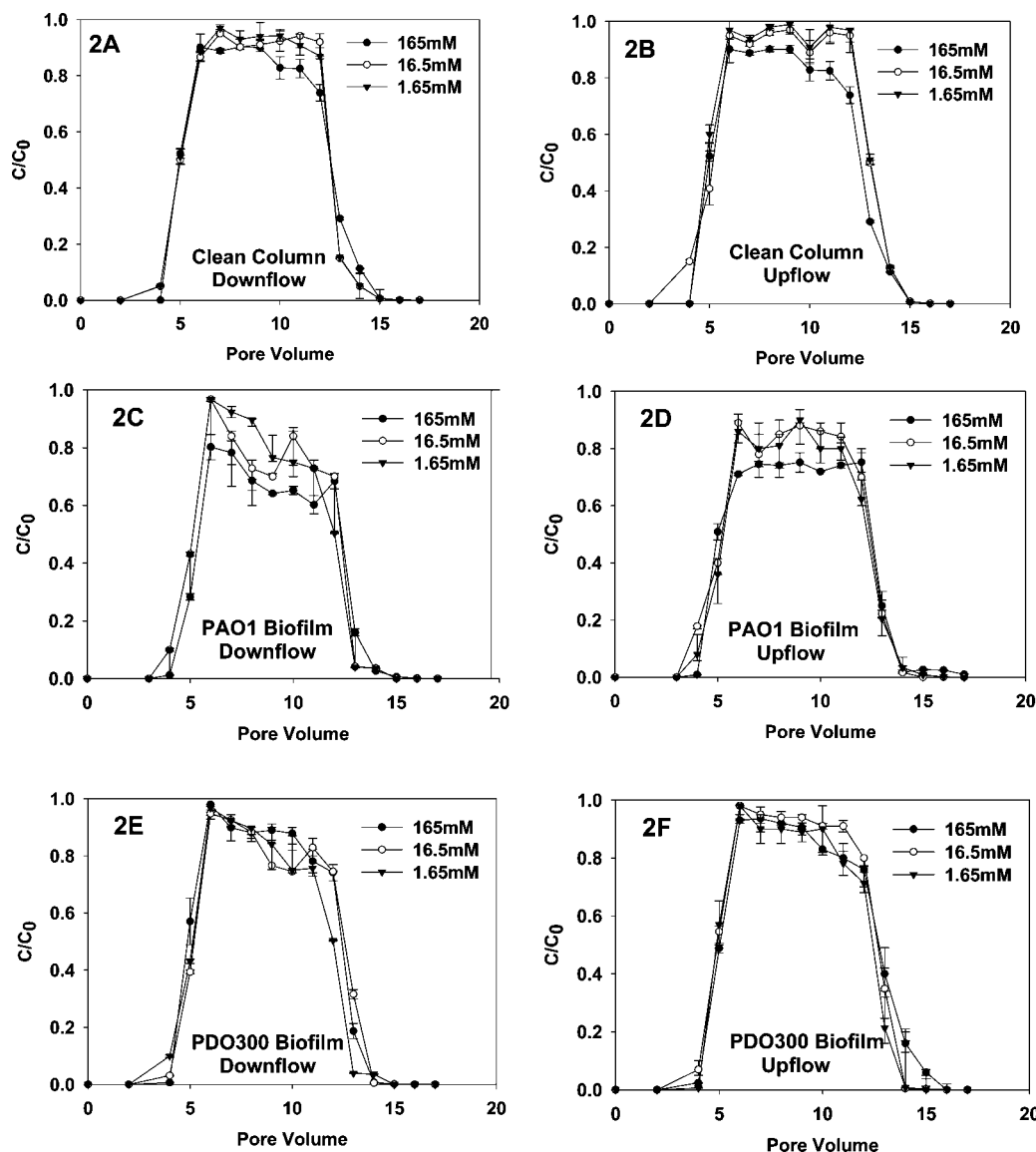


FIGURE 2. Breakthrough curves of Ech3937 in column without biofilm (A and B); column coated with PAO1 biofilm (C and D); and column coated with PDO300 biofilm (E and F) under solution ionic strengths 1.65, 16.5, and 165 mM PBS. Flow of bacterial suspension and background PBS were injected in either downflow direction (A, C, E) or upflow direction (B, D, F). Bacterial injection started at pore volume 3 and ended at pore volume 11. Error bars represent standard deviations of three replicate experiments.

Discussion

Ech3937 Deposition in the Column Section with Thick Biofilm. Significantly higher bacterial retention occurred in the bottom 5 cm of the columns where the majority of the biofilm was found, regardless of flow directions and ionic strength of the carrying solutions. Since the main difference between the bottom 5 cm segment and the rest of the biofilm-coated column is the amount of biomass, we speculate that the extensive biofilm growth in the bottom segment of the column reduced the bed pores and caused the markedly higher k_d observed at the bottom of the columns. These results are in line with a number of other studies that indicated straining could play an important role when the ratio between the particle and median grain diameters is greater than 0.05 (43, 44).

Ech3937 Deposition in the Column Section with Thin Biofilm. Lower k_d was found in the 0–20 cm segments of the biofilm-coated columns, compared with the k_d obtained in the clean column under identical experimental condition, although the overall Ech3937 retention were significantly higher in biofilm-coated columns. This is a strong indication

that the presence of a thin layer of biofilm discouraged Ech3937 adhesion. That decrease of Ech3937 deposition only occurred at places where biofilm thickness was thin suggests that changes in column porosity can be neglected and the physical and chemical properties of the biofilm may be responsible for the impaired bacterial adhesion.

The more negatively charged biofilm EPS compared with the glass bead surfaces may be one of the factors contributing to the decreased deposition of Ech3937 in the top segments of the biofilm-coated column. However, the electrostatic forces between Ech3937 cells and biofilm may not be the controlling factor since the Ech3937 deposition was not affected by the solution ionic strength in PDO300 biofilm-coated columns and PAO1 biofilm-coated columns under low ionic strengths (1.65 and 16.5 mM). Additionally, biofilm surface roughness does not seem to play a significant role in controlling the transport and deposition of Ech3937 in the current experimental system. Previous studies showed that PDO300 biofilms had higher surface roughness than PAO1 biofilms (45, 46). However, our results show that Ech3937 had lower deposition rates in columns coated with PDO300

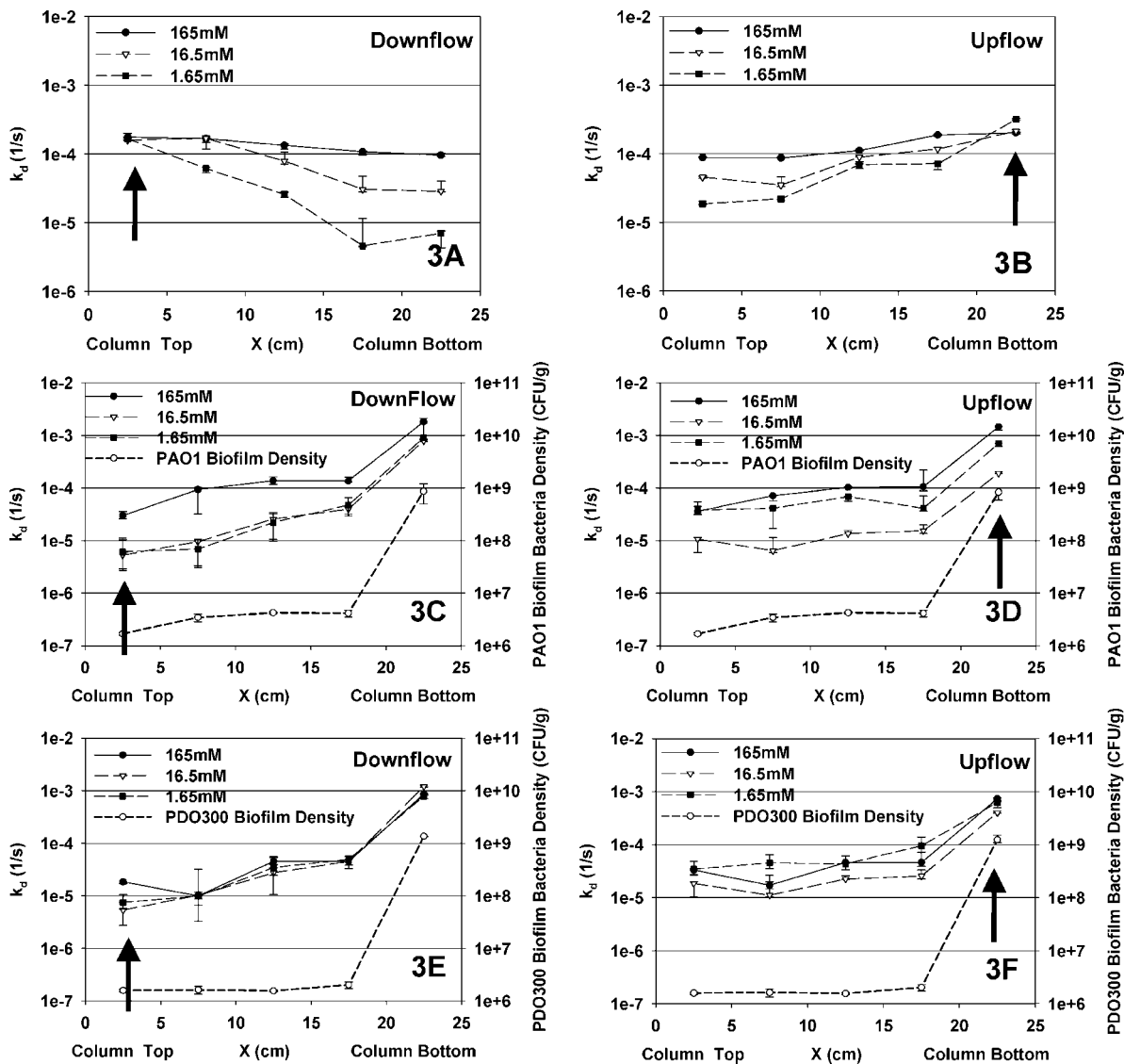


FIGURE 3. Ech3937 deposition coefficient k_d distribution along the bacterial travel distance, in column without biofilm (A and B), column coated with PAO1 biofilm (C and D), and PDO300 biofilm (E and F) under different flow directions, and solution ionic strengths: 1.65, 16.5, and 165 mM PBS. Error bars represent standard deviations of three replicate experiments; arrows indicate the column section close to Ech3937 bacterial injection inlet.

biofilm than in those covered with PAO1 biofilm, despite the fact that greater surface roughness is known to encourage bacterial deposition.

Cell surface hydrophobicity also affect bacterial adhesion (6, 7, 13, 47). When hydrophobic forces are combined with DLVO forces, interaction between the hydrophilic glass beads and hydrophilic Ech3937 cells are repulsive near the solid surface, and Ech3937 may only adhere to the glass beads reversibly at the secondary minimum, depending on the ionic strength. In this study, we were unable to directly measure the surface tension of the *P. aeruginosa* biofilm and bare glass beads; therefore, we cannot exclude the interference from hydrophobicity in Ech3937 cell deposition. Compared with the neutrally charged PAO1 biofilm EPS, the anionic PDO300 EPS may cause higher resistance to Ech3937 bacterial adhesion by incorporating a large amount of water into its structure through hydrogen bonding (48). We speculate this hydration effect may account for the lower adhesion of Ech3937 in the PDO300 biofilm-coated than in the PAO1 biofilm-coated columns.

Another important mechanism that may contribute to the impaired Ech3937 bacterial deposition in biofilm-coated columns is polymer interactions between the bacteria and

biofilm surfaces. Previous research showed that steric interactions can be more important than DLVO-type interactions in explaining bacterial adhesion (7, 9–11). These steric or polymer interactions can be attractive or repulsive, and could extend up to 100 nm compared with the 5 nm of acid–base interaction from the surface into the surrounding (10, 49). Camesano et al. (11) reported that partial removal of extracellular polysaccharides from strains *Pseudomonas putida* KT2442 and *Burkholderia cepacia* G4 resulted in a reduction of the repulsive forces. Jucker et al. (7, 10) also showed that the uneven distribution of short- and long-chain polysaccharides on the bacterial outer surface and the formation of hydrogen bonds could significantly affect bacterial adhesion, and the existence of a dense brush of LPS resulted in low adhesion. Recently, Tong et al. (50) studied the transport of an adhesion-deficient bacterial strain *Comamonas* DA001 in quartz sand and demonstrated that the adhesion deficiency of DA001 was driven by steric interactions from cell surface polymers, resulting in a deviation from log-linear behavior that did not decrease when the energy barrier to deposition was decreased.

In this study, steric interactions may pose repulsive forces between the biofilm-coated column media and suspended

Ech3937 cells, and are responsible for the reduced deposition of Ech3937 in column sections with thin biofilm. The biofilm surface roughness, increased turbulence, and decreased bed porosity are not the controlling mechanisms, which would otherwise encourage Ech3937 deposition in the column.

Impact of Solution Ionic Strength. According to the DLVO theory, increasing the solution ionic strength should monotonically decrease the long-range repulsion between a negatively charged bacterium and a negatively charged surface. There have been a few cases where the expected trend with ionic strength was not seen (11, 51–53). The potential mechanisms for this discrepancy between bacterial attachment and model prediction are bacterial flagella rotation (51), charge regulation (52), ion penetrability (53), and polymer interaction (13). In our study, the deposition of Ech3937 was weakly dependent on the ionic strength only in PDO300 biofilm colonized column media, indicating that PDO300 biofilm surface EPS might be the main mechanism that controls bacterial adhesion. The polysaccharides of PDO300 probably penetrated into the electrostatic barrier region between biofilm surface and Ech3937 cells and thus inhibited deposition throughout the tested ionic strengths.

The main extracellular polysaccharide secreted by PDO300 is alginate, a linear copolymer of mannuronic and guluronic acids (uronic acids $C_6H_{10}O_7$) joined by β 1–4 linkage. Uronic acids are negatively charged and may contribute to the overall negative surface charge of PDO300 cells (5, 54). The primary carbohydrates of the PAO1 EPS are glucose (41.0%), rhamnose (14.3%), and mannose (13.9%), which are neutral sugars and may shield the negatively charged surface functional groups, e.g., LPS and proteins, located on cell membranes (55). For the charged EPS, a decrease in the ionic strength of the solution may change the conformation of the polymers by unfolding and extending them into the solution, as well as changing the “softness” of the polymer layers (11, 13, 16). The extended polymers may provide more sites for reaction with diffused and extended parts of the polymers with the Ech3937 surface than a more collapsed polymer formed in a higher ionic strength solution. An extended polymer also may create a steric repulsive force to any cells approaching the surface. Therefore, the negatively charged alginate of PDO300 biofilm might be responsible for the observed weak correlation between Ech3937 deposition and ionic strength in PDO300 biofilm-coated columns.

Implications. Biofilms are distributed nonuniformly within the natural environment and engineered systems, e.g., there is a marked decrease in biomass with increasing filter depth and corresponding contact time in drinking water and wastewater biofilters. The results presented in this paper demonstrate that biofilm-coated porous media may promote or impair the transport and deposition of bacteria, depending on the thickness of the biofilm and the types of EPS polymer. With thin biofilm accumulation, polymer interaction between the biofilm surface EPS and bacteria plays a more important role in bacterial adhesion while porous media physical and hydrodynamic changes as a result of biofilm growth may become significant when biofilm accumulates to a certain thickness. It should be noted that the observations from this study are based on the model bacteria Ech3937, which is a common gram negative bacteria, but may not represent all bacterial transport conditions since cell surface LPS is known to influence the chemical interactions between bacteria and biofilm.

Acknowledgments

We are thankful to Dr. Sharon Walker and her students for their assistance in measuring the zeta potentials of bacterial strains. We thank three anonymous reviewers for their helpful comments on the manuscript. This work was supported in part by the University of Wisconsin-Milwaukee Graduate

School Fellowship Program, Graduate School Research Committee Award, and Research Growth Initiative.

Supporting Information Available

Figure presenting the influence of solution ionic strength on the zeta potentials of Ech3937, PAO1, and PDO300 bacterial cells, and bare glass beads; tables showing the original k_d data and Ech3937 bacterial recovery mass balance. This material is available free of charge via the Internet at <http://pubs.acs.org>.

Literature Cited

- (1) Denyer, S. P.; Gorman, S. P.; Sussman, M. *Microbial Biofilms: Formation and Control*; Blackwell Scientific Publications: Oxford, 1993.
- (2) Characklis, W. G., Marshall, K. C., Eds. *Biofilms: A Basis for an Interdisciplinary Approach*; Wiley-Interscience: New York, 1990.
- (3) Costerton, J. W.; Lewandowski, Z.; Caldwell, D. E.; Korber, D. R.; Lappin-Scott, H. M. Microbial biofilms. *Annu. Rev. Microbiol.* **1995**, *49*, 711–745.
- (4) Tsuneda, S.; Jung, J.; Hayashi, H.; Aikawa, H.; Hirata, A.; Sasaki, H. Influence of extracellular polymers on electrokinetic properties of heterotrophic bacterial cells examined by soft particle electrophoresis theory. *Colloids Surf., B: Biointerfaces* **2003**, *29*, 181–188.
- (5) Searcy, K. E.; Packman, A. I.; Atwill, E. R.; Harter, T. Capture and retention of *Cryptosporidium parvum* oocysts by *Pseudomonas aeruginosa* biofilm. *Appl. Environ. Microbiol.* **2006**, *72* (9), 6242–6247.
- (6) Salerno, M. B.; Rothstein, S.; Nwachukwu, C.; Shelbi, H.; Velegol, D.; Logan, B. E. Differences between chemisorbed and physisorbed biomolecules on particle deposition to hydrophobic surfaces. *Environ. Sci. Technol.* **2005**, *39* (17), 6371–6377.
- (7) Jucker, B. A.; Harms, H.; Hug, S. J.; Zehnder, A. J. B. Adsorption of bacterial surface polysaccharides on mineral oxides is mediated by hydrogen bonds. *Colloids Surf., B: Biointerfaces* **1997**, *9*, 331–343.
- (8) Tsuneda, S.; Aikawa, H.; Hayashi, H.; Yuasa, A.; Hirata, A. Extracellular polymeric substances responsible for bacterial adhesion onto solid surface. *FEMS Microbiol. Lett.* **2003**, *223*, 287–292.
- (9) Liu, Y.; Yang, C.-H.; Li, J. Influence of extracellular polymeric substances on *Pseudomonas aeruginosa* transport and deposition profiles in porous media. *Environ. Sci. Technol.* **2007**, *41* (1), 198–205.
- (10) Jucker, B. A.; Harms, H.; Zehnder, A. J. B. Polymer interactions between five gram negative bacteria and glass investigated using LPS micelles and vesicles as model systems. *Colloids Surf., B: Biointerfaces* **1998**, *11*, 33–45.
- (11) Camesano, T. A.; Logan, B. E. Probing bacterial electrosteric interactions using atomic force microscopy. *Environ. Sci. Technol.* **2000**, *34*, 3354–3362.
- (12) Prince, J. L.; Dickinson, R. B. Kinetics and forces of adhesion for a pair of capsular/unencapsulated staphylococcus mutant strains. *Langmuir* **2003**, *19*, 154–159.
- (13) Abu-Lail, N. I.; Camesano, T. A. Role of ionic strength on the relationship of biopolymer conformation, DLVO contributions, and steric interactions to bioadhesion of *Pseudomonas putida* KT2422. *Biomacromolecules* **2003**, *4*, 1000–1012.
- (14) Gomez-Suarez, C.; Pasma, J.; van der Borden, A. J.; Wingender, J.; Flemming, H.; Busscher, H. J.; van der Mei, H. C. Influence of extracellular polymeric substances on deposition and re-deposition of *Pseudomonas aeruginosa* to surfaces. *Microbiology* **2002**, *148*, 1161–1169.
- (15) Abu-Lail, N. I.; Camesano, T. A. Role of lipopolysaccharides in the adhesion, retention, and transport of *Escherichia coli* JM109. *Environ. Sci. Technol.* **2003**, *37* (10), 2173–2183.
- (16) Xu, L. C.; Logan, B. E. Interaction forces between colloids and protein-coated surfaces measured using an atomic force microscope. *Environ. Sci. Technol.* **2005**, *39* (10), 3592–3600.
- (17) Xu, L. C.; Logan, B. E. Interaction forces measured using AFM between colloids and surfaces coated with both dextran and protein. *Langmuir* **2006**, *22*, 4720–4727.
- (18) Cunningham, A. B.; Characklis, W. G.; Abedeen, F.; Crawford, D. Influence of biofilm accumulation on porous media hydrodynamics. *Environ. Sci. Technol.* **1991**, *25* (7), 1305–1311.
- (19) Charbonneau, A.; Novakowski, K.; Ross, N. The effect of a biofilm on solute diffusion in fractured porous media. *J. Contam. Hydrol.* **2006**, *85*, 212–228.

- (20) Leon-Morales, C. F.; Leis, A. P.; Strathmann, M.; Flemming, H.-C. Interactions between laponite and microbial biofilms in porous media: implications for colloid transport and biofilm stability. *Water Res.* **2004**, *38*, 3614–3626.
- (21) Vandevivere, P.; Baveye, P. Relationship between transport of bacteria and their clogging efficiency in sand columns. *Appl. Environ. Microbiol.* **1992**, *58* (8), 2523–2530.
- (22) Suhomel, B. J.; Chen, B. M.; Allen, M. B., III. Network model of flow, transport and biofilm effects in porous media. *Transp. Porous Media* **1998**, *30*, 1–23.
- (23) Rockhold, M. L.; Yarwood, R. R.; Niemet, M. R.; Bottomley, P. J.; Selker, J. S. Considerations for modeling bacterial-induced changes in hydraulic properties of variably saturated porous media. *Adv. Water Res.* **2002**, *25*, 477–495.
- (24) Chatterjee, A. K.; Starr, M. P. Genetics of *Erwinia* species. *Annu. Rev. Microbiol.* **1980**, *34*, 645–676.
- (25) Rahme, L. G.; Ausubel, F. M.; Cao, H.; Drenkard, E.; Goumnerov, B. C.; Lau, G. W.; Mahajan-Miklos, S.; Plotnikova, J.; Tan, M.-W.; Tsongalis, J.; Walendziewicz, C. L.; Tompkins, R. G. Plants and animals share functionally common bacterial virulence factors. *Proc. Natl. Acad. Sci.* **2002**, *97*, 8815–8821.
- (26) Pier, G. B.; Grout, M.; Zaidi, T. S.; Olsen, J. C.; Johnson, L. G.; Yankaskas, J. R.; Goldberg, J. B. Role of mutant CFTR in hypersusceptibility of cystic fibrosis patients to lung infections. *Science* **1996**, *271*, 64–67.
- (27) Cho, J. J.; Schroth, M. N.; Kominos, S. D.; Green, S. K. Ornamental plants as carriers of *Pseudomonas aeruginosa*. *Phytopathology* **1975**, *65*, 425–431.
- (28) Li, J.; McLellan, S.; Ogawa, S. Accumulation and fate of green fluorescent labeled *Escherichia coli* in laboratory-scale drinking water biofilters. *Water Res.* **2006**, *40* (16), 3023–3028.
- (29) Liu, Y.; Li, J.; Qiu, X.; Burda, C. Bactericidal activity of nitrogen-doped metal oxides nanocatalysts and influence of bacterial extracellular polymeric substances (EPS). *J. Photochem. Photobiol., A* **2007**, *190*, 94–100.
- (30) Miller, W. G.; Leveau, J. H.; Lindow, S. E. Improved *gfp* and *inaZ* broad-host-range promoter-probe vectors. *Mol. Plant-Microbe Interact.* **2002**, *13*, 1243–1250.
- (31) Peng, Q.; Yang, S.; Charkowski, A. O.; Yap, M.-N.; Steeber, D. A.; Keen, N. T.; Yang, C.-H. Population behavior analysis of *dspE* and *pelD* regulation in *Erwinia chrysanthemi* 3937. *Mol. Plant-Microbe Interact.* **2006**, *19*, 451–457.
- (32) Brown, M. J.; Lester, J. N. Comparison of bacterial extracellular polymer extraction methods. *Appl. Environ. Microbiol.* **1980**, *40*, 179–185.
- (33) Dubois, M.; Gilles, K. A.; Hamilton, J. K.; Rebers, P. A.; Smith, F. Colorimetric method for determination of sugars and related substances. *Anal. Chem.* **1956**, *28* (3), 350–356.
- (34) Filisertti-Cozzian, T. M. C. C.; Carpital, N. C. Measurement of uronic acids without interference from neutral sugars. *Anal. Biochem.* **1991**, *197*, 157–162.
- (35) Iwasaki, T. J. Some notes on sand filtration. *Am. Water Works Assoc.* **1937**, *29* (10), 1591–1602.
- (36) Tufenkji, N.; Redman, J. A.; Elimelech, M. Interpreting deposition patterns of microbial particles in laboratory-scale column experiments. *Environ. Sci. Technol.* **2003**, *37* (3), 616–623.
- (37) Yao, K. M.; Habibiyan, M. T.; O'Melia, C. R. Water and wastewater filtration: concepts and applications. *Environ. Sci. Technol.* **1971**, *5* (11), 1105–1112.
- (38) Li, X.; Scheibe, T. D.; Johnson, W. P. Apparent decreases in colloid deposition rate coefficient with distance of transport under unfavorable deposition conditions: a general phenomenon. *Environ. Sci. Technol.* **2004**, *38* (21), 5616–5625.
- (39) Tufenkji, N.; Elimelech, M. Breakdown of colloid filtration theory: role of the secondary energy minimum and surface charge heterogeneities. *Langmuir* **2005**, *21*, 841–852.
- (40) Tong, M.; Johnson, M. P. Colloid population heterogeneity drives hyperexponential deviation from classic filtration theory. *Environ. Sci. Technol.* **2007**, *41*, 493–499.
- (41) Simoni, S. F.; Harms, H.; Bosma, T. N. P.; Zehnder, A. J. B. Population heterogeneity affects transport of bacteria through sand columns at low flow rates. *Environ. Sci. Technol.* **1998**, *32* (14), 2100–2105.
- (42) Redman, J. A.; Grant, S. B.; Olson, T. M.; Estes, M. K. Pathogen filtration, heterogeneity, and the potable reuse of wastewater. *Environ. Sci. Technol.* **2001**, *35* (9), 1798–1805.
- (43) Bradford, S. A.; Yates, S. R.; Bettahar, M.; Simunek, J. Physical factors affecting the transport and fate of colloids in saturated porous media. *Water Resour. Res.* **2002**, *38* (12), 1327; doi: 10.1029/2002WR001340, 63.1–63.12.
- (44) Bradford, S. A.; Simunek, J.; Bettahar, M.; Tadassa, Y. F.; van Genuchten, M. T.; Yates, S. R. Straining of colloids at textural interfaces. *Water Resour. Res.* **2005**, *41*; W10404, doi: 10.1029/2004WR003675.
- (45) Hentzer, M.; Teitzel, G. M.; Balzer, G. J.; Heydorn, A.; Molin, S.; Givskov, M.; Parsek, M. R. Alginate overproduction affects *Pseudomonas aeruginosa* biofilm structure and function. *J. Bacteriol.* **2001**, *183* (18), 5395–5401.
- (46) Stapper, A. P.; Narasimhan, G.; Ohman, D. E.; Barakat, J.; Hentzer, M.; Molin, S.; Kharazmi, A.; Hoiby, N.; Mathee, K. Alginate production affects *Pseudomonas aeruginosa* biofilm development and architecture, but is not essential for biofilm formation. *J. Med. Microbiol.* **2004**, *53*, 679–690.
- (47) Rijnaarts, H. H. M.; Norde, W.; Bouwer, E.; Lyklema, J.; Zehnder, A. J. B. Bacterial deposition in porous media: effects of cell-coating, substratum hydrophobicity, and electrolyte concentration. *Environ. Sci. Technol.* **1996**, *30*, 2877–2883.
- (48) Pringle, J. H.; Fletcher, M. Influence of substratum hydration and adsorbed macromolecules on bacterial attachment to surfaces. *Appl. Environ. Microbiol.* **1986**, *51* (6), 1321–1325.
- (49) Meinders, J. M.; van der Mei, H. C.; Busscher, H. J. Deposition efficiency and reversibility of bacterial adhesion under flow. *J. Colloid Interface Sci.* **1995**, *176*, 329–341.
- (50) Tong, M.; Li, X.; Brow, C.; Johnson, W. P. Detachment-influenced transport of an adhesion-deficient bacterial strain within water-reactive porous media. *Environ. Sci. Technol.* **2005**, *39* (8), 2500–2508.
- (51) McClaine, J. W.; Ford, R. M. Reversal of flagellar rotation is important in initial attachment of *Escherichia coli* to glass in a dynamic system with high- and low-ionic-strength buffers. *Appl. Environ. Microbiol.* **2002**, *68*, 1280–1289.
- (52) Dan, N. The effect of charge regulation on cell adhesion to substrates: salt-induced repulsion. *Colloids Surf., B: Biointerfaces* **2003**, *27*, 41–47.
- (53) Poortinga, A. T.; Bos, R.; Busscher, H. J. Electrostatic interactions in the adhesion of an ion-penetrable and ion-impenetrable bacterial strain to glass. *Colloids Surf., B: Biointerfaces* **2001**, *20*, 105–117.
- (54) Frank, B. P.; Belfort, G. Polysaccharides and sticky membrane surfaces: critical ionic effects. *J. Membr. Sci.* **2003**, *212*, 205–212.
- (55) Wozniak, D. J.; Wyckoff, T. J. O.; Starkey, M.; Keyser, R.; Azadi, P.; O'Toole, G. A.; Parsek, M. R. Alginate is not a significant component of the extracellular polysaccharide matrix of PA14 and PAO1 *Pseudomonas aeruginosa* biofilms. *Proc. Natl. Acad. Sci.* **2003**, *100* (13), 7907–7912.

ES071698K